



Stability Improvement of Methylammonium Lead Iodide Perovskite Thin Films by Bismuth Doping

JULIA MARÍ-GUAITA,¹ AMAL BOUICH ^{1,2} and BERNABÉ MARÍ¹

1.—Institut de Disseny per a la Fabricació i Producció Automatitzada, Universitat Politècnica de València, Valencia, Spain. 2.—e-mail: bouich.amal@gmail.com

Perovskites have been in the spotlight in the field of solar cells due to their high efficiency and their low cost of materials and fabrication processes. Perovskite solar cells (PSCs) have shown an efficiency of up to 25%. Nevertheless, PSCs have some drawbacks such as rapid degradation in ambient conditions. To improve PSC stability, lead is usually replaced with bismuth. In this article, we report the results when doping the methylammonium lead iodide ($\text{CH}_3\text{NH}_3\text{PbI}_3$, aka MAPbI_3), with different bismuth quantities. The incorporation of bismuth into the lattice leads to a remarkable change in optoelectronics and morphological structure. Substituting lead atoms with 2% bismuth improves some characteristics of MAPbI_3 layers, such as removing pinholes and increasing crystallite size and optical absorption. Furthermore, bismuth doping improves the stability of pure MAPbI_3 layers, which after 4 weeks exhibits higher degradation compared to bismuth-doped MAPbI_3 samples, which remain stable after that period.

INTRODUCTION

It is known worldwide that photovoltaic solar energy (PSE) is experiencing remarkable growth as it is an excellent source of renewable energy. PSE has the potential to offer a significant supply of globally demanded energy. Every hour of sun radiation that the Earth receives could be enough to produce enough electricity for a whole year of the world requirements.

Perovskites, used as absorbers in photovoltaic solar cells, have shown exceptional optical and electronic properties as well as substantial reductions in the manufacturing costs and ease of fabrication. However, perovskites have some drawbacks when used in solar cells, and they experience rapid degradation when exposed to UV radiation. The new generation of mixed organic-inorganic halide perovskites is promising in PSE because they have successfully shown efficiencies over 25% when using perovskite absorbers in solar cells.¹

Solar cell performance depends highly on the perovskite layer, which is responsible for the light absorption and generation of photoinduced carriers. Therefore, perovskite layers need delicate and critical deposition when fabricating the solar cell. Hybrid perovskites, described with the formula ABX_3 (where A is a cation such as Cs or CH_3NH_3 , B is usually lead, and X is halide) can be fabricated by different methods; one-step and two-step spin-coatings are the most used solution processes for the perovskite layers. One-step spin-coating deposition stands out over two-step for its ease of fabrication.

Among all hybrid-organic-inorganic-perovskites, methylammonium lead iodide $\text{CH}_3\text{NH}_3\text{PbI}_3$ (MAPbI_3) seems to be one the best options for solar cells due to its outstanding ferroelectric, pyroelectric, fibroelastic, and piezoelectric properties, and they have also been reported to be excellent absorber layers in solar cells with a 15% increase of efficiency in only 4 years.²

Bismuth (Bi) doping was used to overcome the inconvenience of toxicity and degradation of MAPbI_3 solar cells. It enhanced the rate of degradation of hybrid organic-inorganic perovskites by the partial substitution of Pb by Bi.³ In addition,

recent studies on Bi-doped MAPbI₃ perovskite reported high defect tolerance, improved Seebeck coefficient, and higher electrical conductivity.⁴

In other research works, Cs cation has been used to substitute MA in the MAPbI₃ structure to investigate its potential for solar cells. XRD (x-ray diffraction) showed that when incorporating Cs in the MAPbI₃, the tetragonal structure is transformed to an orthorhombic phase. Also, when adding Cs, the connectivity of the grains increases, and, with 40 and 50% Cs doping, the inter-grain voids are improved in the films resulting in better performance and major photoconversion efficiency (PCE) of the photovoltaic devices when adding enough Cs.⁵

Many studies have focused on doping of MAPbI₃ to improve the efficiency of perovskite solar cells (PSCs). Few studies use Mg as a doping agent. It is known that Mg could be interesting to incorporate into the MAPbI₃ perovskites because it affects the energy band structure and morphology.⁶

Calcium was also used as a doping agent for MAPbI₃. The addition of Ca enlarges bandgap structures by concurrent up-shifting. Besides, the electronegativity of Ca is smaller than that of Pb, and the stronger antibonding character Ca-I bonding results in a larger bandgap of Ca²⁺ perovskite. Moreover, Lu et al. concluded that doping the MAPbI₃ with Ca is a highly effective strategy to improve the photovoltaic performance of solar cells.⁷

Recent studies reported that Cl-doped MAPbI₃ improves the charge transport within the perovskite layer substantially. This may be essential for obtaining good photovoltaic efficiencies.⁸

When doping the MAPbI₃ with Rb, the conductivity of the perovskite could be significantly tuned from *n*-type to *p*-type. The carrier concentration and mobility can be controlled by the dopant concentration. In addition, a slight blue shift of the photoluminescence (PL) peak was reported with the increase of Rb, and at the concentration range of 1.5–1.8 M, the dominant crystal structure can go from cubic to orthorhombic.⁹

In this work, we doped MAPbI₃ perovskites with different bismuth percentages to explore how doping with bismuth affects the properties of the perovskite films. Bismuth ions incorporated in MAPbI₃ thin films improve the crystallinity of MAPbI₃ layers and enhance the electrical properties of the device. Furthermore, as the Bi atom has a similar radius to Pb, it is relatively easy to incorporate Bi into the MAPbI₃ lattice by substituting the Pb atom.¹⁰ The synthesis of the Bi-doped MAPbI₃ samples was performed by the one-step spin method. After the synthesis, the samples prepared were characterized with different techniques such as XRD, field emission scanning electron microscope (FESEM), atomic force microscopy (AFM), PL, and optical absorbance to establish the crucial parameters for excellent performance in perovskite-based devices. We report that bismuth doping intensifies the properties of MAPbI₃,

allowing better electrical performance and especially improving the stability of MAPbI₃-based solar cells after 4 weeks under dark.

EXPERIMENTAL PROCEDURE

Materials

All chemicals used were bought from Sigma-Aldrich and used as received. Methylammonium iodide (MAI), lead iodide (PbI₂, 99%), and bismuth (III) iodide (BiI₃, 99%) were used as precursor materials, and dimethylformamide (DMF 99.9%) and dimethyl sulfoxide (DMSO 99.9%) as solvents.

Elaboration of Thin Films

MAPbI₃ thin films were deposited on fluorine tin oxide (FTO)-coated glass substrates. The FTO substrates were cleaned for 15 min in Hellmanex detergent, ethanol, acetone, and isopropanol in an ultrasonic bath and subsequently exposed for 15 min to ambient UV-ozone.

MAPbI₃ precursor solution was prepared by completely dissolving MAI and lead iodide in dimethyl sulfoxide (DMSO) (0.095 mL) and dimethyl formamide (DMF) 1 mL, at room temperature. To dope MAPbI₃ with bismuth, a variable amount (*x*%) of bismuth iodide was added, where *x* is the percentage of Bismuth present in the starting solution. The solution prepared was left to heat overnight at 75 °C in the glovebox. FTO substrates were statically spin-coated at 4500 RPM for 50 s, after which they were annealed for 5 min at 50 degrees and then 10 min for 100 degrees. Samples were kept in an inert N₂ atmosphere until used.

Figure 1 displays the preparation process of the samples. In (a) the solutions with different quantities of bismuth are placed over the plate to be completely dissolved. In (b) we can see the substrates of FTO (2.5 cm × 2.5 cm) where we will deposit the different solutions. In (c) there is the scheme of how we deposit the solution on the substrate in the spin-coating machine. Finally, (d) shows pictures of the samples prepared after the annealing treatment.

Characterization Techniques

In the samples studied for this work, MAPbI₃ thin films doped with different quantities (0%, 1%, 2%, 4%, and 8%) of bismuth were characterized by XRD using a RIGAKU Ultima IV diffractometer with Cu *k*α radiation (*λ* = 1.5418 Å). Morphology images were taken with FESEM Quanta 200-FEI at 1.5 kV applied voltage; AFM measurements were performed by Nano Surf Mobile S microscope scanning using tapping mode. Optical properties were performed with Ocean Optics HR4000 spectrophotometer by a Si-CCD, and PL emission source was a semiconductor laser at 405 nm.

RESULTS AND DISCUSSION

The different samples, MAPbI₃ undoped and doped with the different bismuth (Bi) doping percentages $x\%$ where ($x = 0, 1, 2, 4, 8$), were scanned with XRD analysis as shown in Fig. 2a. The diffraction peaks located at 14.0, 24.0, 28.0, and 32.0 correspond to the planes of (110), (211), (220), (222), (400), and (303), respectively, that belong to the characteristic peaks of MAPbI₃. The peaks reported correspond to the same diffraction peaks previously reported.^{9,10} Furthermore, the incorporation of Bi contents from (0–8%) shows an improvement in the MAPbI₃ peak intensity where 2%Bi sample shows slightly higher intensity than the rest of the samples, and a decrease was observed for PbI₂ peaks, which indicated the enhanced stability of doped MAPbI₃. These results are well matched with the previously reported pure MAPbI₃ crystalline phase. As indicated by XRD, the bi-doped MAPbI₃ single crystals maintain a perfect cubic perovskite structure (Pm-3m).¹¹

Figure 2b shows the calculated crystallite size for the characteristic peaks (110) and (220) of XRD peaks. The graph shows that, for both peaks, the crystallite size decreases when increasing the amount of bismuth added to the starting solution. This trend is more evident for peak 220 than for peak 110. However, the position of both XRD peaks

seems to be independent of the amount of bismuth. This fact is due to the similar ionic radius of lead and bismuth.

The surface morphology and roughness vary with the different quantities of bismuth in the perovskite thin films. These parameters are shown in Table I. Effective lattice strain has been calculated to determine the deformations of the grains in the surface of the film. Equation 1 was used to obtain the effective lattice strain (ε).¹²

$$\beta \cos(\theta) = \frac{k\lambda}{D} + 4\varepsilon \sin(\theta) \quad (1)$$

where θ is the Bragg angle, k is a constant (0.94), β is the full width half maximum (FWHM), and λ is the wavelength of the x-ray. The dislocation density of the crystal was calculated using Eq. 2.

$$\delta = \frac{1}{D^2} \quad (2)$$

To verify how the morphology changes MAPbI₃, pure films are observed by doping with bismuth, FESEM analysis of pure MAPbI₃, and doped $x\%$ Bi, where x (0, 1, 2, 4, 8) was performed. Figure 3 shows top-view FESEM images of the different samples analyzed in the work. The surface of the 1% bismuth sample looks quite like the pure MAPbI₃. According to the grain size, we report a bigger grain size when the percentage of bismuth in the sample is higher.

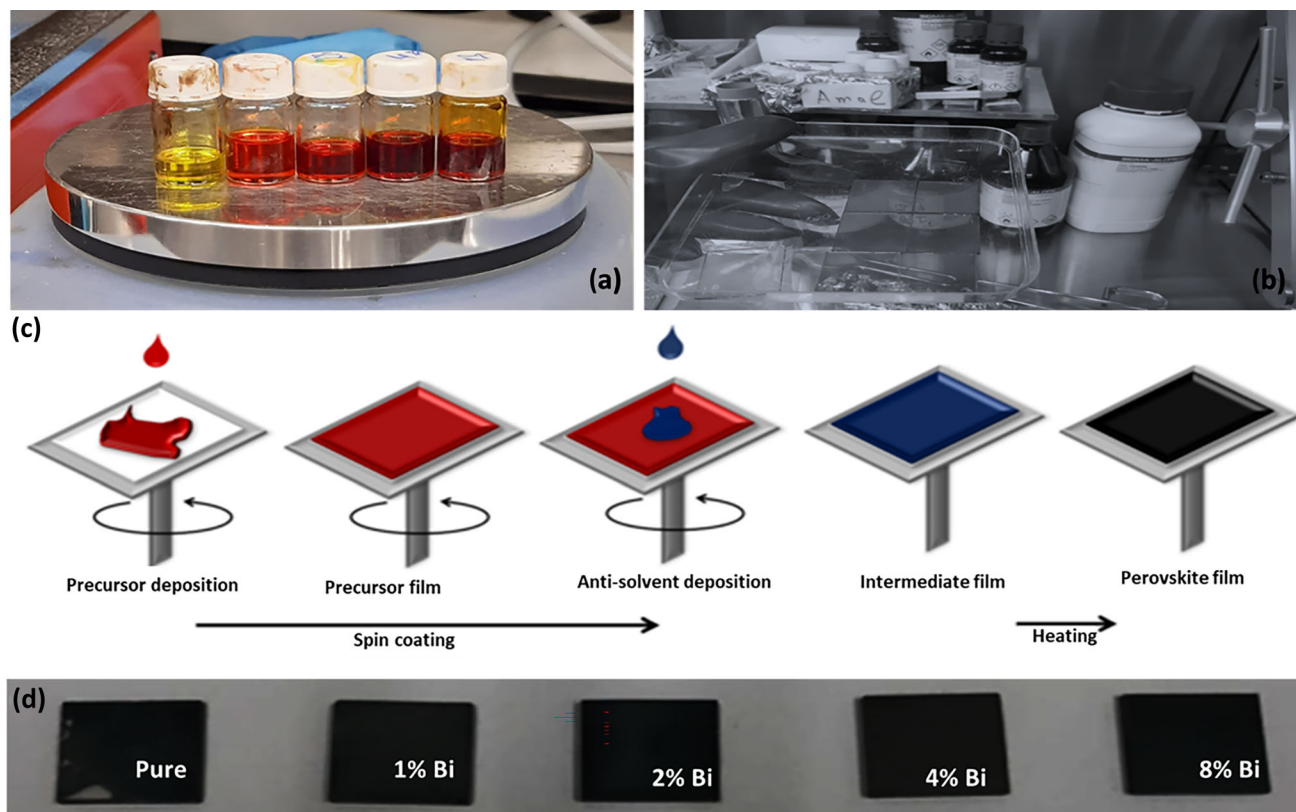


Fig. 1. Scheme of the one-step spin-coating procedure for thin film MAPbI₃ perovskites.

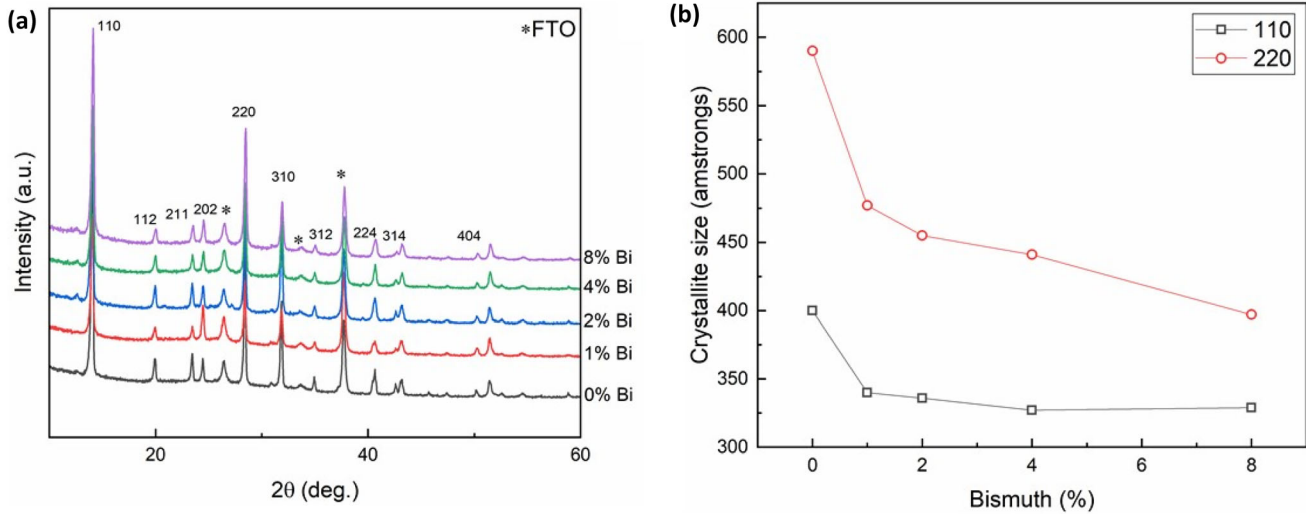


Fig. 2. (a) XRD patterns of MAPbI₃ pure and doped $x\%$ Bi where x (0, 1, 2, 4, 8). (b) Crystallite size of characteristic 110 and 220 XRD peaks for different amounts of Bi.

Table I. Grain size, dislocation density, and lattice strain of XRD of MAPbI₃ thin films

Sample ID	Grain size (nm)	Roughness (nm)	Dislocation density (nm ⁻¹)	Lattice strain ($\epsilon \times 10^{-3}$)
Pure MAPbI ₃	333	145	0.90×10^{-5}	9.05
2% Bi	345	420	0.84×10^{-5}	8.71
8% Bi	293	231	1.16×10^{-5}	8.13

Also, 4% bismuth sample and 8% bismuth sample have dark surfaces and are not as smooth as 1% and 2% samples. The FESEM image of the MAPbI₃ coincides with the work of Chen et al. where they report the morphology of the MAPbI₃.¹³ Also, mapping analysis shows that lead and iodide were distributed homogenously in the surface of pure MAPbI₃ (Fig. 3f–h).

The MAPbI₃ surface contained irregularly sized grain boundaries; the 1% Bi-doped makes the film surface homogeneous with the reduction of the size of the grain boundary. Moreover, the crystal and grain sizes are noticeably increased with 2% Bi.

The absorption study was performed to understand the impact of bismuth on the optical properties of MAPbI₃. All the samples prepared show good absorption with a small difference between the samples by increasing the percentage of Bi dopant, and the absorption of the pure sample (MAPbI₃) agrees with the previously reported paper.¹⁴ Figure 4a shows the absorbance for undoped and doped MAPbI₃ layers with different amounts of Bi. The absorption onset for all samples is located at about 800 nm, except for 2 and 4%Bi doping, which seems to shift to higher wavelengths; 2% Bi sample shows slightly higher absorption than the rest of the

samples, matching also with the FESEM results above; this indicates better performance of the perovskite film.

The photoluminescence measurements shown in Fig. 5 were recorded at ambient temperature. We report that the PL peak intensity for the different bismuth percentages is in the range of 700–850 nm. Also, we report the highest PL peak intensity is in 2% of the bismuth sample compared to the PL peak of pure MAPbI₃ and MAPbI₃ doped with 8% bismuth. The higher intensity of PL indicates good photoluminescent properties of the prepared films.

Figure 6 shows the AFM analysis of the perovskite thin films of pure MAPbI₃, MAPbI₃ doped with 2% Bi, and MAPbI₃ doped with 8% Bi in a $2 \mu\text{m} \times 2 \mu\text{m}$ area. According to the experimental analysis carried out at the AFM, roughness and surface morphology of the different samples vary with the amount of bismuth present in the absorber layer, showing that 2% of the bismuth sample has R_{rms} of 420 nm and grain size of 345 nm (see Table II), which is greater compared with pure MAPbI₃ and 8% bismuth samples.

According to Table II, the dislocation density of these three samples was studied intensely because it shows better characterization and varies between

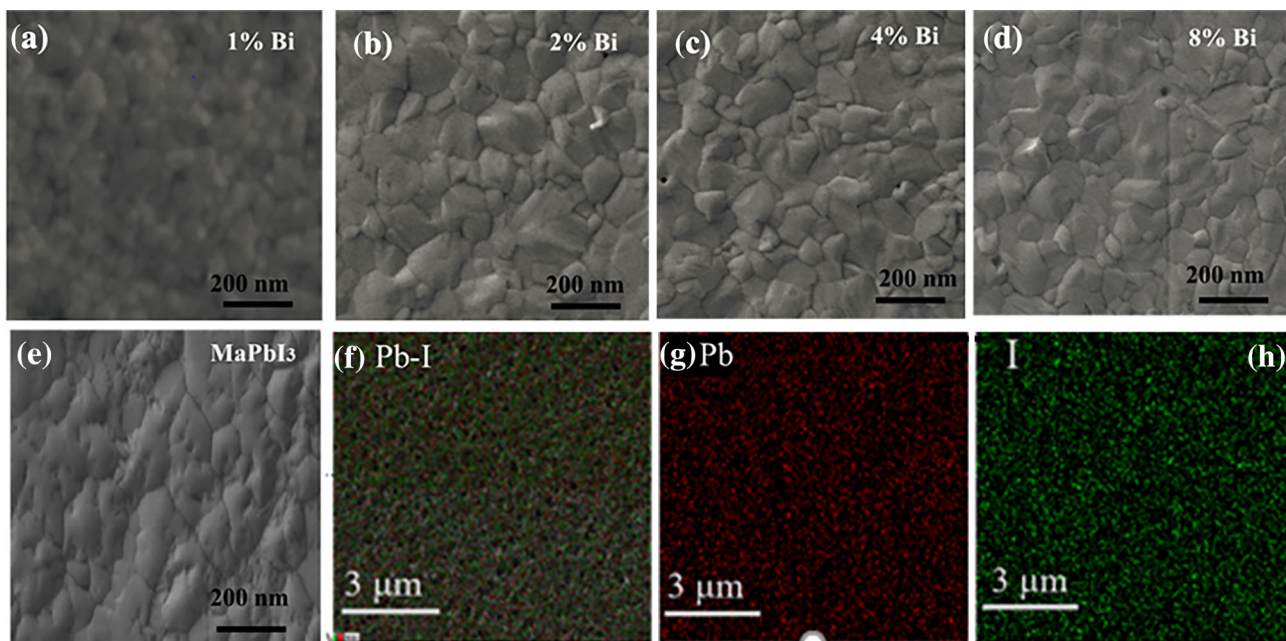


Fig. 3. (a)–(e) FESEM images of MAPbI₃ thin films doped with different percentages of Bi ($x = 0, 1, 2, 4, 8$). (f)–(h) Mapping of Pb and I components in halide perovskite MAPbI₃.

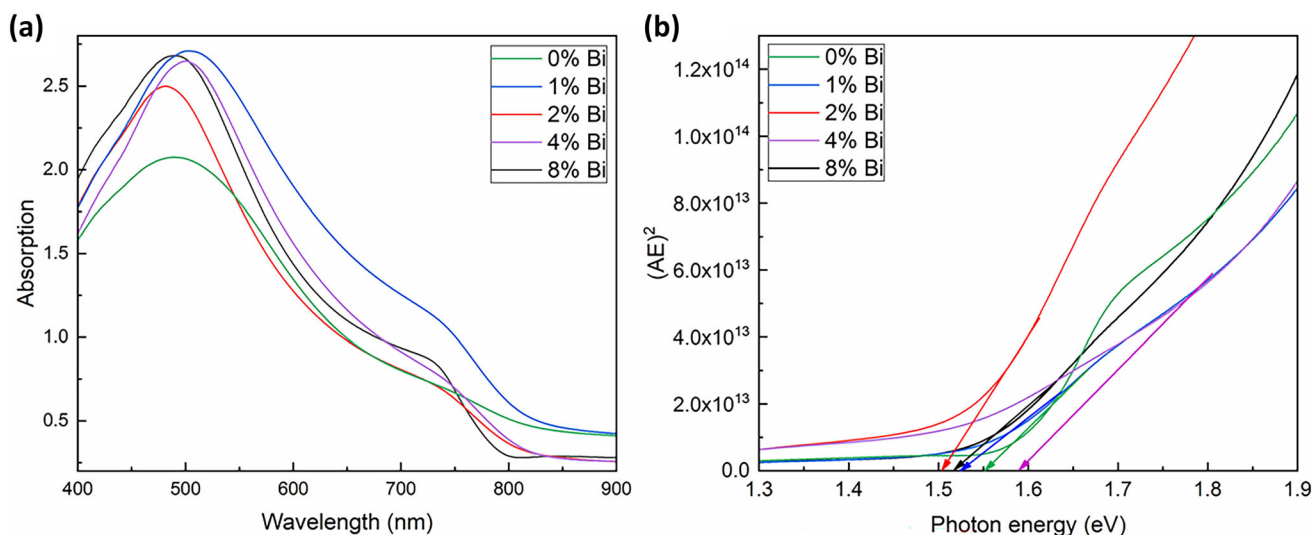


Fig. 4. (a) UV-visible absorption of MAPbI₃ thin films doped with different percentages of Bi (x (%) = 0, 1, 2, 4, 8). (b) Optical bandgap of MAPbI₃ thin films doped with different percentages of Bi (x (%) = 0, 1, 2, 4, 8). (b) $(A \cdot E)^2$ versus the energy photons, which is the standard way to calculate the value of the optical bandgap. The UV visible technique is from 1.5 eV to 1.55 eV as shown in Table I where the MAPbI₃ doped 2% bismuth samples have the optimal bandgap around 1.50 eV.

$0.84 \times 10^{-5} \text{ nm}^{-1}$ and $1.16 \times 10^{-5} \text{ nm}^{-1}$. Lower dislocation density means better performance, which means that in this case the 2% bismuth sample is the better option although it does not show higher effective lattice strain.

DEGRADATION STUDY

Perovskite solar cells are vulnerable to oxygen and humidity.^{15,16} In this study, bismuth is used to overcome this rapid degradation. The prepared samples were kept in dark ambient conditions for 1 week. When samples were kept in dark ambient

conditions, they did not experience degradation at all for 1 week. Therefore, we can confirm that bismuth improves the stability of the samples that started showing degradation after week 4. After 5 weeks, the samples of 2%, 4%, and 8% bismuth kept under in the dark remained stable (see Fig. 7b).

As mentioned before, the sample that showed better performance in all the characterization parts was the one prepared with 2% bismuth. In Fig. 7a,

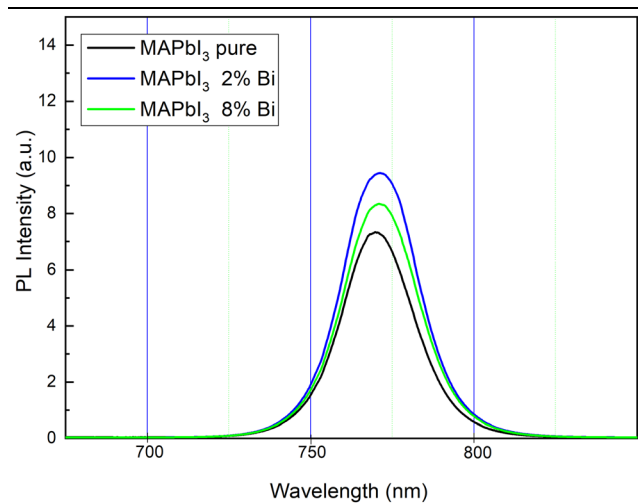


Fig. 5. Room temperature photoluminescence of perovskite thin films; pure MAPbI₃ and BMAPbI₃-Bi, with 2% and 8% bismuth.

we can see an evolution of the optical bandgap of the 2%Bi sample where the bandgap of the aged Bi sample remained good after 4 weeks.^{17–20} This means this quantity of bismuth enhances the performance and stability of the film well. To sum up, we report that bismuth plays an important role in slowing down the degradation of MAPbI₃ thin films.

CONCLUSION

In this study, we present the result of different perovskite absorbers with different quantities of bismuth as a doping agent to improve the stability and the performance of optoelectronic devices. The different samples were prepared inside a glovebox through a one-step spin coating method and subsequently characterized by XRD, FESEM, optical absorption, and photoluminescence. XRD study indicates that the addition of Bi increases the intensity of the MAPbI₃ diffraction peaks, with the 2% Bi specimen being the sample with the highest XRD intensity and the lowest presence of PbI₂ peaks, which is a signal of the improved stability of Bi-doped MAPbI₃ thin films. The crystallite size graph reveals that, for the characteristic peaks of the perovskite compound, the crystallite size decreases when the quantity of bismuth added to the starting solution is higher because of the bigger size of the ionic radius of lead in relation to bismuth. FESEM images show grain sizes are notably

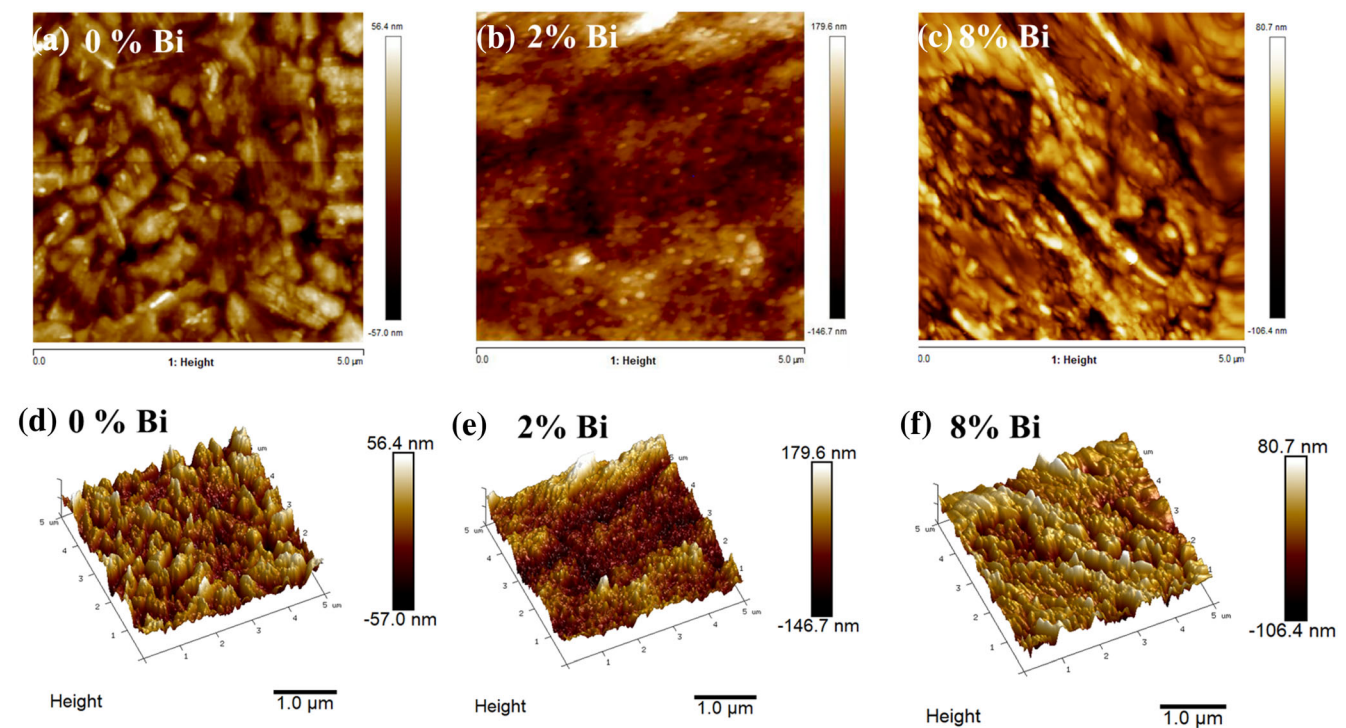


Fig. 6. (a) Two-dimensional AFM image of MAPbI₃; (b) 2D AFM images of MAPbI₃ thin films doped with 2% Bi. (c) Two-dimensional AFM images of MAPbI₃ thin films doped with 8% Bi. (d) Three-dimensional AFM image of MAPbI₃; (e) 3D AFM images of MAPbI₃ thin films doped with 2% Bi; (f) 3D AFM images of MAPbI₃ thin films doped with 8% Bi.

Table II. Optical properties of MAPbI₃ thin films doped with different percentages of Bi

Sample ID	Optical bandgap by absorption		Emission PL peak		Stokes shift (meV)
	λ_c (nm)	Eg (eV)	λ (nm)	Eg (eV)	
Pure MAPbI ₃	719	1.55	760	1.40	150
2% Bi	795	1.50	770	1.35	150
8% Bi	752	1.53	768	1.36	180

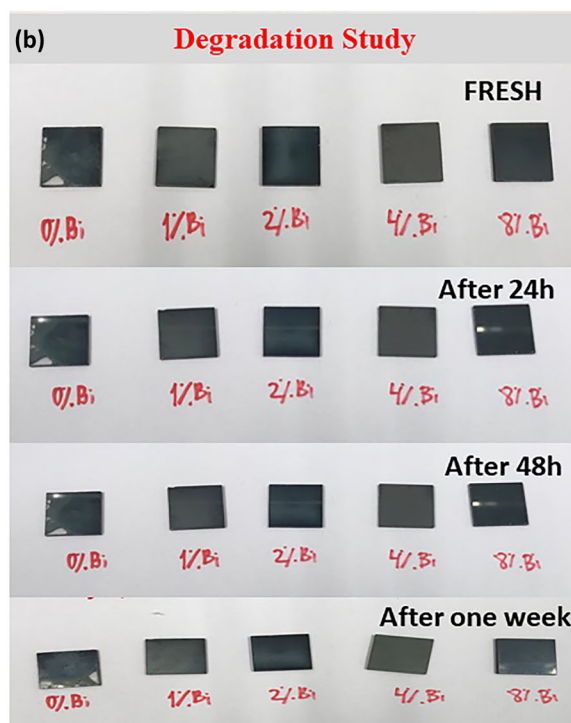
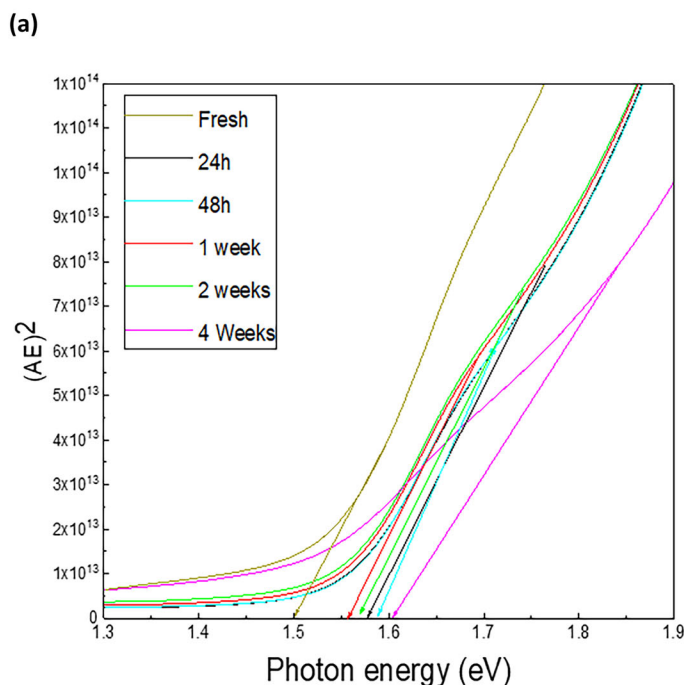


Fig. 7. (a) Optical bandgap of MAPbI₃ thin films doped with 2% bismuth for different periods after the deposition. (b) Degradation study of samples with different bismuth percentages along time.

improved when adding 2% bismuth to the MAPbI₃, which means better performance in photovoltaic devices.

ACKNOWLEDGEMENTS

This work was supported by Grant PID2019-107137RB-C21 funded by MCIN/AEI/10.13039/501100011033 and by “ERDF: A way of making Europe.” Author Dr. Amal Bouich acknowledges the post-doctoral contract supported by the RRHH and the postdoctoral contract of the Margarita Salas financed with European Union Next Generation.

FUNDING

Open Access funding provided thanks to the CRUE-CSIC agreement with Springer Nature.

CONFLICT OF INTEREST

The authors declare that they have no known competing financial interests or personal relation-

ships that could have appeared to influence the work reported in this paper.

OPEN ACCESS

This article is licensed under a Creative Commons Attribution 4.0 International License, which permits use, sharing, adaptation, distribution and reproduction in any medium or format, as long as you give appropriate credit to the original author(s) and the source, provide a link to the Creative Commons licence, and indicate if changes were made. The images or other third party material in this article are included in the article's Creative Commons licence, unless indicated otherwise in a credit line to the material. If material is not included in the article's Creative Commons licence and your intended use is not permitted by statutory regulation or exceeds the permitted use, you will need to obtain permission directly from the copyright holder. To view a copy of this licence, visit <http://creativecommons.org/licenses/by/4.0/>.

REFERENCES

1. J.J. Yoo, G. Seo, M.R. Chua, T.G. Park, Y. Lu, F. Roter-mund, and J. Seo, *Nature* 590, 587 (2021).
2. A. Bouich, B. Mari, L. Atourki, S. Ullah, and M.E. Touhami, *JOM* 73, 551 (2021).
3. T.D. Siegler, D.W. Houck, S.H. Cho, D.J. Milliron, and B.A. Korgel, *J. Phys. Chem. C* 123, 963 (2018).
4. J. Bartolomé, E. Climent-Pascual, C. Redondo-Obispo, C. Zaldo, A.L. Álvarez, A. de Andrés, and C. Coya, *Chem. Mater.* 31, 3662 (2019).
5. M. Imran, A. Saleem, N.A. Khan, and A.H. Kamboh, *Physica B* 572, 1 (2019).
6. F. Yang, M.A. Kamarudin, G. Kapil, D. Hirotani, P. Zhang, C.H. Ng, and S. Hayase, *ACS Appl. Mater. Interfaces* 10, 24543 (2018).
7. C. Lu, J. Zhang, D. Hou, X. Gan, H. Sun, Z. Zeng, and Y. Zhu, *Appl. Phys. Lett.* 112, 193901. (2018).
8. S. Colella, E. Mosconi, P. Fedeli, A. Listorti, F. Gazza, F. Orlandi, and R. Mosca, *Chem. Mater.* 25, 4613 (2013).
9. X. Bai, X. Zou, J. Zhu, Y. Pei, Y. Yang, W. Jin, and D. Chen, *Mater. Lett.* 211, 328 (2018).
10. C. Li, X. Chen, N. Li, J. Liu, B. Yuan, Y. Li, and B. Cao, *J. Mater. Chem. C* 8, 3694 (2020).
11. X. Guo, C. McCleese, C. Kolodziej, A.C. Samia, Y. Zhao, and C. Burda, *Dalton Trans.* 45, 3806 (2016).
12. Bouich, A., Ullah, S., Ullah, H., Mollar, M., Marí, B., and Touhami, M.E., *JOM* 72, 615 (2020).
13. Y. Xiong, L. Xu, P. Wu, L. Sun, and G. Xie, Hu, B. *Adv. Funct. Mater.* 29, 1900615 (2019).
14. C. Bi, Y. Shao, Y. Yuan, Z. Xiao, C. Wang, Y. Gao, and J. Huang, *J. Mater. Chem. A* 2, 18508 (2014).
15. A. Bouich, J. Marí-Guaita, B. Sahraoui, P. Palacios, and B. Marí, *Front. Energy Res.* 10, 840817 (2022).
16. A. Bouich, J. Marí-Guaita, A. Bouich, I.G. Pradas, and B. Marí, *Eng. Proc.* 12, 81 (2022).
17. J. Marí-Guaita, A. Bouich, M.A. Shafi, A. Bouich, and B. Marí, *Phys. Status Solidi A* 219, 2100664 (2022).
18. S. Ullah, A. Bouich, H. Ullah, B. Mari, and M. Mollar, *Sol. Energy* 208, 637 (2020).
19. K. Fradi, A. Bouich, B. Slimi, and R. Chtourou, *Optik* 249, 168283 (2022).
20. J. Marí-Guaita, A. Bouich, and B. Marí, *Eng. Proc.* 12, 1 (2021).

Publisher's Note Springer Nature remains neutral with regard to jurisdictional claims in published maps and institutional affiliations.